Microgels of silylated HPMC as a multimodal system for drug co-encapsulation

Mohamed Zayed, Corine Tourné-Péteilh, Michel Ramonda, Gildas Réthoré, Pierre Weiss, Jean Martinez, Gilles Subra, Ahmad Mehdi, Jean-Marie Devoisselle, Philippe P. Legrand

▶ **To cite this version:**

Mohamed Zayed, Corine Tourné-Péteilh, Michel Ramonda, Gildas Réthoré, Pierre Weiss, et al.. Microgels of silylated HPMC as a multimodal system for drug co-encapsulation. International Journal of Pharmaceutics, 2017, 532 (2), pp.790 - 801. 10.1016/j.ijpharm.2017.07.074 . hal-01620498

HAL Id: hal-01620498
https://hal.science/hal-01620498

Submitted on 5 Mar 2021

HAL is a multi-disciplinary open access archive for the deposit and dissemination of scientific research documents, whether they are published or not. The documents may come from teaching and research institutions in France or abroad, or from public or private research centers.

L'archive ouverte pluridisciplinaire **HAL**, est destinée au dépôt et à la diffusion de documents scientifiques de niveau recherche, publiés ou non, émanant des établissements d'enseignement et de recherche français ou étrangers, des laboratoires publics ou privés.

*Manuscript revised version
Click here to view linked References

Microgels of silylated HPMC as a multimodal system for drug co-encapsulation

Mohamed ZAYED[1], Corine TOURNE-PETEILH*[1], Michel RAMONDA[4], Gildas RETHORE [3], Pierre WEISS[3], Jean MARTINEZ [2], Gilles SUBRA[2], Ahmad MEHDI[1], Jean-Marie DEVOISSELLE[1], Philippe LEGRAND[1]

[1] Institut Charles Gerhardt Montpellier, UMR 5253 CNRS-UM-ENSCM, Place Eugène Bataillon, 34095 Montpellier Cedex 5, France

[2] Institut de Biomécules Max Mousseron, UMR 5247 UM-CNRS- ENSCM, Faculté de Pharmacie, 15 Av. Charles Flahault BP 14 491, 34093 Montpellier Cedex 5, France

[3] Inserm, U1229, Regenerative Medicine and Skeleton Research, RMeS, Nantes, France - Université de Nantes, UFR Odontologie, Nantes, France - CHU Nantes, PHU 4 OTONN, Nantes, France.

[4] Centrale de Technologie en Micro et nanoélectronique, Université Montpellier, 860 rue de Saint Priest, 34097 Montpellier, France

Abstract

Combined therapy is a global strategy developed to prevent drug resistance in cancer and infectious diseases. In this field, there is a need of multifunctional drug delivery systems able to co-encapsulate small drug molecules, peptides, proteins, associated to targeting functions, nanoparticles. Silylated hydrogels are alkoxysilane hybrid polymers that can be engaged in a sol−gel process, providing chemical cross linking in physiological conditions, and functionalized biocompatible hybrid materials.

In the present work, microgels were prepared with silylated (hydroxypropyl)methyl cellulose (Si-HPMC) that was chemically cross linked in soft conditions of pH and temperature. They were

prepared by an emulsion templating process, water in oil (W/O), as microreactors where the condensation reaction took place.

The ability to functionalize the microgels, so-called FMGs, in a one-pot process, was evaluated by grafting a silylated hydrophilic model drug, fluorescein (Si-Fluor), using the same reaction of condensation. Biphasic microgels (BPMGs) were prepared to evaluate their potential to encapsulate lipophilic model drug (Nile red). They were composed of two separate compartments, one oily phase (sesame oil) trapped in the cross linked Si-HPMC hydrophilic phase.

The FMGs and BPMGs were characterized by different microscopic techniques (optic, epi-fluorescence, Confocal Laser Scanning Microscopy and scanning electronic microscopy), the mechanical properties were monitored using nano indentation by Atomic Force Microscopy (AFM), and different preliminary tests were performed to evaluate their chemical and physical stability.

Finally, it was demonstrated that it is possible to co-encapsulate both hydrophilic and hydrophobic drugs, in silylated microgels, that were physically and chemically stable. They were obtained by chemical cross linking in soft conditions, and without surfactant addition during the emulsification process. The amount of drug loaded was in favor of further biological activity. Mechanical stimulations should be necessary to trigger drug release.

Key words: Microgels, Sol-Gel, alkoxysilane functionalization, co-encapsulation.

1. Introduction

Combined therapies gather a wide field of applications where drugs have to be co-encapsulated, to overcome drug resistance in cancer treatments (Borcoman, Le Tourneau, 2016; Bradshaw, Sobel, 2016; Teo, *et al.*, 2016), infectious diseases (Le Douce, *et al.*, 2016; Bento da Silva, *et al.*, 2016), and surgical diseases (Morgan et al., 2016), or to combine growth factor action in tissue regeneration (Subbiah, *et al.*, 2015). Targeted delivery or theranostic approaches could also be combined with drug controlled release providing one dose drug delivery systems (Ulbrich, *et al.*, 2016; Kelkar,

Reineke, 2011). So, there is a potential and challenging benefit to design multimodal injectable drug delivery systems embedding complementary activities and/or combining cell surface functions such as ligands, adhesion molecules, cytokines, growth factors. One of the limitations of these approaches is to take into account all together the therapeutic goals as well as the formulation constraints. Another limitation is the multi-step building chemistry process used to functionalize nano/ microparticles. Such designs need multi-process and multi-functional approaches. In this context, there is a need of new functionalized polymers to embed different complementary activities, which respects biocompatibility, but also reduces the time, the cost, and the environmental impact of the manufacturing process.

Microgels are defined as microparticles of chemical (covalent links) or physical (weak interactions) cross linked hydrogels. They consist of three-dimensional polymer network, able to swell or shrink under large amount of water exchanges. They could be responsive to the changes in pH, temperature or other physiological stimuli, suitable for drug controlled release. They are basically obtained and stabilized by hydrogen-bond or electrostatic interactions in alginate (Matalanis, *et al.*, 2011), chitosan (Dang, *et al.*, 2016), and pectine. (Marquis, *et al.*, 2014) Nevertheless for some applications, chemical cross linking could be recommended to improve the mechanical properties, stabilize the drug interactions and prevent burst release effects. (Zhao, 2013)

For decades hydrogels have been investigated to design delivery systems for Active Pharmaceutical Ingredients (APIs). They are composed of natural or synthetic polymers that could be cross linked by chemical covalent bonds, or physically *via* non-covalent links, in order to form a network able to control the API delivery. (Pagels, 2015) Physical cross linked hydrogels are usually obtained by weak ionic interactions, in ionisable polymers such as hyaluronic acid, pectin, chitosan and alginate. (Hamidi, *et al.*, 2008) Chemical hydrogels are obtained by covalent cross linking most of the time using polymers modified with methacrylate derivatives (Hamidi, *et al.*, 2008; Jagadeesan, *et al.*, 2011; Nguyen, *et al.*, 2015; Cha, *et al.*, 2014; Bachman, *et al.*, 2015; Glaubitz, *et al.*, 2014), or using cross linking reagents such as gluteraldehyde, carbodiimides, or di-halo species (Pagels,

Prud'homme, 2015). The presence of such species and/or the formation of bypass products during the cross linking reaction, could interact with biological environment and disturb the cell metabolism.

Recently, a new family of hydrogels were functionalized with alkoxysilane groups, allowing chemical cross linking, based on the hydrolysis condensation reaction of -$Si(OR)_3$ into stable Si-O-Si covalent links. Thus, silylated (hydroxypropyl)methyl cellulose (Si-HMPC) were developed as biocompatible and injectable silylated hydrogels (Bourges, *et al.*, 2002a, 2002b; Echalier, *et al.*, 2016; Vinatier, *et al.,* 2009; Vinatier, *et al*., 2007; Vinatier, *et al*., 2009; Liu, *et al.*, 2014). Interestingly, bisilylated poly(ethylene glycol) (Si-PEG) was also synthesized and exhibits relevant cytotoxicity results (Echalier, *et al*., 2016). Then, Si-hydrogels open up a wide range of applications including bone repair (Zhang, *et al.*, 2016; Struillou, *et al.*, 2013), cartilage tissue engineering (Buchtova, *et al.*, 2013), and treatment of chronic colonic diseases (Moussa, *et al*., 2017). Echalier *et al.* has developed Si-peptides hydrogels leading to biological responsive hydrogels such as adhesive peptide sequence RGD, peptide sequence having antibacterial activity (Echalier, *et al*., 2016) or collagen inspired (Echalier, *et al.*, 2017).

To the best of our knowledge, there is no example of microgels obtained with silylated hydrogels, and little examples of chemical microgels bearing lipidic compartments for co-encapsulation of complementary APIs. Jagadeesan *et al.* have trapped hexadecane droplets in an aqueous phase containing a monomer n-isopropylacrylamide, a cross linker N,N'-methylenebis(acrylamide) a surfactant Brij 35), and a photoinitiator 2,2'-azobis (2-methylpropionamidine) dihydrochloride. (Jagadeesan, *et al*, 2011) Recently Busatto *et al*. proposed oil in hyaluronic acid microgels for enzymatic trigger release of an hydrophobic drug (progesterone). (Busatto, *et al*., 2017) Whatever the emulsification strategies, encapsulation of lipophilic components remains a complex task because of the stabilization of the O/W primary emulsion (Matalanis, *et al*., 2013) and may require approaches such as Pickering emulsions. (Marquis, *et al.*, 2016)

105 The aim of this work was to (i) demonstrate the ability to produce microgels using silylated HPMC
106 by the way of the Sol-Gel reaction of condensation of the -SiOR functions, (ii) to functionalize them,
107 with a model function, using the same Sol-Gel reaction in a one-pot process (FMGs), and (iii) to
108 generate biphasic microgels (BPMGs) containing lipophilic compartments intended to formulate
109 poorly soluble drugs. Model drugs were used in the present work, Nile Red (NR) as lipophilic and
110 silylated Fluorescein (Si-Fluor) as chemically linked function.
111
112 **2. Materials and methods**
113
114 **2.1. Materials**
115
116 Silylated (hydroxypropyl)methyl cellulose (Si-HPMC) (MM = 290 000 $g.mol^{-1}$) was obtained as
117 previously described (Bourges, *et al*., 2002b) by grafting 0.6 wt% of 3-glycidoxy-
118 propyltrimethoxysilane on E4M® grade cellulose in heterogeneous medium. It was used in its
119 hydrolyzed form at 3 wt.% in 0.2M NaOH that was done under constant stirring for 48 h and
120 sterilized by steam (121°C, 30 min). (Vinatier, *et al.,* 2007) Si-Fluor was obtained as previously
121 described (Ciccione, *et al*., 2016) using 25 mg of fluorescein isothiocyanate stirred with 500 µL of
122 dimethyl sulfoxide (DMSO) and 3-aminopropyltriethoxysilane for 2 h in the dark at room
123 temperature and used without further purification. A mother solution was used at 170 mM in ethanol
124 and stored at -20°C for months. Refined sesame oil was purchased from Cooper (Melun, Franc. Nile
125 red (NR) was obtained from Sigma Aldrich chemie GmbH (France), MM = 318.3 g/mol, and Lutrol
126 F-127 from BASF (Ludwigshaffen, Germany).
127
128 **2.2. Preparation of the functionalized microgels (FMGs)**
129
130 The W/O emulsion was obtained after the addition of the Si-HPMC solution into the oily phase. It
131 was added to the sesame oil with a controlled feeding rate of 0.1 mL/min, using a syringe pump
132 apparatus (HARVARD APPARATUS pump 33), at a ratio of 1/10 v:v. The dispersion was done

under high shearing stress using a disperser (Disperser T18 digital ULTRA-TURRAX), with a 10 mm rotor-stator, IKA®-WERK GmbH & Co. KG (Staufen, Germany) at a speed of 5000 rpm in ice for 20 min. Then, the temperature was increased to 45°C and maintained for 10 min. The dispersion was left to stand overnight at room temperature under mild stirring (500 rpm) for aging. Finally, FMGs were washed with H_2O/ethanol (1/1 v:v) and stabilized with 0.05% Lutrol F-127, an injectable surfactant, to facilitate the suspension handling.

The aqueous phase was composed of 1 mL of Si-HPMC solution 3 wt.%, that was neutralized with 2-[4-(2-hydroxyethyl)piperazin-1-yl]ethane sulfonic acid buffer (HEPES, PM = 238,3 g/mol) at pH 3.5, with a volume ratio of 1:2 (Vinatier, *et al*., 2007). The Si-HPMC hydrogel was functionalized by Si-Fluor ethanolic solution that was added to the Si-HPMC phase, and kept in ice. The mixture was diluted two times with fresh sesame oil to reduce the aggregation of the microgels.

2.3. Preparation of the biphasic microgels (BPMGs)

A O/W primary emulsion was obtained by dispersing the sesame oil solution of NR (Ultra Turrax, 5000 rpm for 1 min) in the Si-HPMC solution with a volumic ratio of 5%. The Si-HPMC continuous phase was then neutralized and maintained in ice. To prepare the BPMGs, the O/W primary emulsion was dispersed in the sesame oil continuous phase (O/W/O) with a syringe pumps apparatus (HARVARD APPARATUS pump 33). The feeding rate was optimized in the range of 0.1 to 1 mL/min. The final volume ratio was 1/10. After this step, the process was the same as for FMGs.

2.4. Interfacial tension and rheological properties

The surface and interfacial tension were measured with a Krüss tensiometer K100 using the Wilhelmy plate method. The experiments were performed at room temperature (20-25°C) in aqueous solution of Si-HPMC in the range 0.03 wt.% and 3.75×10^{-6} wt.%.

159 The dynamic viscosity of the continuous phase was measured with a coaxial cylinder rheometer,
160 Rheomat RM 200 (Lamy, France) at 7.7°C, 21.0°C, 38.0°C and 48.0 °C. The velocity, ω, was
161 continuously increased from 64.6 to 1290.0 s^{-1}. The force exerted on the cylinder (diameter 30 mm)
162 was measured and converted to a shear stress.
163
164 **2.5. FMGs and BPMGs Characterizations**

165 The optical characterizations were performed by Epi-fluorescence microscopy on an inverted EVOS
166 ® FL, Life Technologies, laser scanning confocal microscope (LSCM) was done on a Confocal Leica
167 SP8. The scanning electronic microscopy (SEM) was done on a MEB FEI Quanta 200 environmental,
168 for the observation of the as-synthesized microgels, as well as the freeze-dried samples.
169
170 The size distribution of the FMGs, BPMGs and oil droplets were achieved with the Image J program.
171 The size was measured for at least 100 items as possible, with $n \geq 20$, and by using at least two
172 different photos. The size distribution was graphically expressed in percentage number of particles
173 and fitted by the Log Normal function were x_c gave the mean size and w the standard deviation
174 (OriginPro 8.1).

175 **2.6. Nano indentation and topographic analysis by AFM**

176 Study of the nanomechanical properties of the FMGs and BPMGs and the scanning
177 topographically of its surface was done by atomic force microscope (AFM D3100 Bruker
178 Instruments), with a Nanoscope 3A Quadrex (electronics device) in which the mode
179 contact was used without scanning (fixed point to perform approach retract curve). The tip
180 has a platinium coverage (around 10 nm) and on the apex of a lever there are point probe
181 nanosensors with a nominal spring constant 0,4N/m (measured with thermal tune). The tip
182 is mounted on a tip-holder suitable for measurement on liquid environment. The
183 measurement of the Force, F (N), to indentation distance, δ (m), were done on hydrated
184 microgels, whose surface was totally dried before applying the AFM to prevent attachment

of the microgels to the tip of the cantilever. The Young's elastic modulus, E (Pa), was calculated after linearization of the equation of the Sneddon model:

$$F = \frac{2}{\pi} \frac{E}{(1 - \upsilon^2)} \tan(\alpha)\, \delta^2$$

with the Poisson's ratio, ν = 0.5, the half angle of the indenter, α = 35°. The topographic observations were done after drying the samples under air overnight.

2.7. Determination of the amount of Si-Fluor linked to cross linked Si-HPMC

The amount of Si-FITC which was covalently linked, C_L, , was evaluated in bulk Si-HPMC gels, at different initial concentrations (C_i). The bulk Si-HPMC gels were with 0.100 mL of a solution of Si-HPMC 3 wt.% that was neutralized by HEPES pH 3.5. After 2 days of aging, the bulk gels were washed consequently with two saline solutions. Firstly, the bulk gels were washed with Phosphate Buffer Solution (PBS) at pH 7.4 and room temperature, to remove the free Si-FITC not chemically linked or weakly adsorbed to the Si-HPMC (C_{Ads}). Secondly, the gels were soaked in NaOH 0.2 M pH 10. These hydrolytic conditions led to the cleavage of the Si-O-Si bonds, and allowed to extract the chemically linked species or the one less adsorbed but not extracted in PBS (C_H). Then, a full extraction was done by Dimethyl Sulfoxide (C_{DMSO}). The amount of FITC extracted were determined by spectrofluorimetry (spectrofluorimeter RF 5000, Shimadzu) at λ_{ex}= 490 nm and λ_{em}= 515 nm. The concentration of strongly linked species (C_L) was calculated according to the following equation:

$$C_L = C_i - (C_{Ads} + C_{DMSO} + C_H)$$

2.8. Chemical and physical stability of FMGs and BPMGs

The stability of FMGs and BPMGs was evaluated in different media and followed by means of dosage of Nile Red (NR) and fluorescein, microscopic observations and their mechanical properties. 20 mg of FMGs or BPMGs were introduced into 50 mL of each medium, namely (i) in physiological simulated media, that is in Phosphate Buffer Saline (PBS) 66 mM at pH 7.4 and in HCl medium at

209 pH 1.5 for 40 days at 37°C, (ii) in alkaline hydrolytic conditions in 0.2 M NaOH at pH 10 for 1 hour
210 at room temperature, and (iii) in Dimethyl Sulfoxide (DMSO) for full extraction.

211 Samples were taken at different times and measured on the spectrofluorimeter (RF 5000, Shimadzu),
212 using λ_{ex}=551 nm and λ_{em} = 609 nm to detect the NR, and λ_{ex} = 490 nm and λ_{em} = 515 nm for
213 fluorescein.

214 **3. Results and discussion**

215

216 **3.1. Preparation of the microgels**

217

218 The microgels were obtained using an emulsion-templating method that produces water in oil
219 droplets, acting as microreactors, where the cross linking reaction could take place. As previously
220 shown by P. Weiss and co-workers, the cross linking of Si-HPMC was done in soft conditions, with a
221 maximum rate of condensation of the silanolate functions into siloxane bridges at pH 7.4 and a
222 temperature of 45°C (Fatimi, Tassin, 2009). As suggested by the authors, the gelation time increased
223 as a function of temperature which has a catalytic action on the condensation reaction. They suggest
224 also that, at high temperature (45°C or higher), additional mechanisms, such as the association of the
225 hydrophobic zones in the polysaccharide chain, can reinforce the essential network formation
226 process.

227

228 This reaction was adapted to occur in the microreactors, containing the Si-HPMC hydrogel solution,
229 in its alkaline form, $-SiO^-Na^+$ and the buffer for the neutralization. To obtain the narrower size
230 distribution and the more spherical microparticles, different parameters were carefully tuned in order
231 to separate in time the dispersion of the water phase and the reaction of condensation. The whole
232 optimizations were done on the preparation of the BPMGs. Scheme 1 summarizes the principal of the
233 formation of the functionalized microgels with the silylated fluorescein (FMGs) and the biphasic
234 microgels (BPMGs), thanks to the critical physico-chemical parameters involved in the process.

235

First of all, the W/O emulsion formed a microenvironment at which the condensation reaction could take place. This step was common to both the preparation of the FMGs and the BPMGs, and was the critical step to obtain the microgels. Indeed, it required the emulsion stability and the kinetic control of the condensation reaction. The first point was insured by the unique intrinsic interfacial properties of HPMC to stabilize the W/O emulsion. Indeed, aqueous solutions of Si-HPMC and HPMC exhibited similar interfacial liquid/air activities, Γ, critical aggregation concentrations, CAC, and Gibbs surface areas, A_{Gibbs} (Table 1) (Wollenweber, *et al*., 2000). The mean interfacial tensions, $\gamma_{o/w}$, between water and sesame oil were measured at 35.2 mN/m and was significantly decreased in presence of Si-HPMC at 14.8 mN/N, allowing to stabilize the emulsion interface. Then, it was possible to obtain stable emulsions without addition of extra surfactant or other chemical modification to decrease the interfacial tension (Figure 1A, D).

Secondly, because of the kinetic aspect of the condensation reaction, the emulsification step has to be carefully separated from the cross linking initiation during the preparation process. Indeed, as the pH neutralization lead to the condensation of silanolate groups, even at room temperature, and form the three dimensional network in about 15 min (Fatimi, Tassin, 2009), the W/O preparations were done below 10°C, to delay the condensation reaction. Moreover, high shearing rate dispersion was applied to favor the formation of the microreactors during the water phase dispersion. Hence, the condensation reaction led to a strong increase of the dynamic viscosity, η_{disp}, of dispersed aqueous phase, from 2000 Pa.s (pH 12-13, 20°C) to 20000 Pa.s (pH 7, 45°C), while it tend to slightly decrease in the continuous phase from η_{cont} = 69 Pa.s to 30 Pa.s, respectively. In these conditions the ratio $\eta_{disp}/\eta_{cont} >> 1$, so that a high shearing stress was necessary to split the dispersed aqueous phase into microdroplets before the cross linking occurred. When the temperature was increased up to 45°C, the condensation reaction was induced.

Figure 1B shows that the formation of the microgels was only done in presence of the siloxane functions, after induction of the condensation by tuning both the pH and the temperature. Si-HPMC precipitations (Figure 1C) may appear even without these stimulations, but with no control of the

morphology. Furthermore, the formation of the Si-O-Si bridges contributed to the stability of the W/O emulsion, as no droplets could be found at the end of the process when native HPMC was used (Figure1E).

Finally, the feeding rate of the water phase was optimized because it was found to be a limiting factor to obtain spherical, non-aggregated microgels with controlled size distribution. The optimized microparticles were obtained for a feeding rate of 0.1 mL/min of O/W emulsion added to the oily phase as shown in Figure 2. The size distribution of the microgels was centered at 46.0 µm (STD = 0.2; $r^2 = 0.95$). When they are filled of oil droplets, BPMGs, it was centered at 72.6 µm (STD = 0.3; $r^2 = 0.84$). Here a compromise had to be done between the mean size and the distribution width.

3.2. Evaluation of the functionalization potential of the microgels (FMGs)

Fluorescein isothiocyanate modified by silanization (Si-Fluor) (Echalier, *et al*., 2016) was chemically linked to the free siloxanes functions of the Si-HPMC polymer chains of the microgels during the cross linking reaction, in a one-pot process. It could be noticed that no toxic catalyzer such as sodium fluoride (usually applied to catalyze sol-gel reactions) was used in this process as it could be necessary for the linking of Si-Fluor in Si-PEG hydrogels even at low concentration respecting the cell viability (Echalier, *et al*., 2016). That represents a great advantage against cytotoxicity and purification steps.

Different consecutive extraction steps were applied to the bulk Si-HPMC gels in order to estimate the maximum amount of Si-FITC, C_L, which could be strongly linked to the silylated polymer (Table 2). It was calculated depending on the equation $C_L = C_i - (C_{Ads} + C_{DMSO} + C_H)$. The amount of covalently linked Si-FITC was obtained by subtracting from the initial concentration of Si-FITC (C_i), the sum of the free Si-FITC weakly adsorbed to the Si-HPMC (C_{Ads}), the chemically linked less stable species (C_H) and the amount extracted by DMSO (C_{DMSO}). DMSO is an organic solvent that could solubilize all the species present, without any effect on the Si-O-Si covalent link.

A maximum of 1.12 µg of Si-FITC per gram of Si-HPMC was covalently linked, as no Si-FITC could be detected in the PBS medium, meaning that the whole Si-FITC species added were totally linked. This represents about 70 µmole of FITC per 1 mole of HPMC, taking into account a total of siloxanes functions available in the hydrogel estimated to 0.6 wt%. (Fatimi, *et al.*, 2008)

These amounts are in good agreement with biological activities usually expected or observed, and comprises in the pM to µM range of concentrations in interactions (Popp, *et al*., 2017), cells adhesion (Wu *et al*., 2017), cancer therapy (Rui, *et al*., 2017), or antibody recognition. (Colombo *et al*., 2016)

3.3. Biphasic microgels (BPMGs) preparation and Nile Red loading efficiency

BPMGs were produced by following a two steps O/W/O emulsion templating process. The W/O emulsion templating step was the same as for the production of the FMGs. Here we describe the formation of the primary emulsion O/W that was used as a reservoir for the lipophilic model drug. Figure 3 shows a microscopic description of a homogeneous primary O/W emulsion. The size distribution of the oil droplets was sharpened and centered to 4.0 µm with a STD of 0.15 determined by the log normal fitting curve. After freeze drying, the oil droplets were still trapped in the Si-HPMC matrix (Figure 3D) in the same size range observed in primary emulsion O/W. These results gave an evidence of the emulsion stability using the interfacial activity of the HPMC, that simplify the chemical composition of continuous phase, usually requiring hydrophilic surfactant (Jagadeesan, *et al*., 2011) or nanoparticles in Pickering O/W emulsions. (Marquis, *et al*., 2016)

SEM observations of the as-synthesized and freeze-dried BPMGs gave the proof that the oil droplets were still trapped inside the Si-HPMC network (Figure 4) as it was observed in the freeze dried O/W primary emulsion (Figure 3). The oil droplets were uniformly distributed in whole volume of the BPMGs as shown by LSCM observations (Figure 4C). The internal texture of the Si-HPMC matrix exhibited fibers of the cellulosic network, that had a diameter in the range of 10 nm. It formed a porous network of a mean ladder distance of 20 nm determined on the topographic picture obtained by AFM (Figure 4D).

Nile red (NR) was chosen as a model drug because its log P value comprises between 3.0 and 5.0 (Küchler, *et al*., 2009; Merian, *et al*., 2012; Weber, *et al*., 2014) which is the value of 30 to 40 % of the commercialized APIs (lipophilic to low lipophilic) covering a wide range of applications. (Pyka, *et al*., 2006; Pallicer, *et al*., 2014) Sesame oil was selected because of its good solubilization power for poorly soluble drugs (Ahmed, Hassan, 2007). It is injectable for subcutaneous or intramuscular administration and it is used as a constituent for the preparation of multiple-emulsion formulation. (Rowe, *et al*., 2009) NR was directly loaded in the primary O/W emulsion up to saturation in the sesame oil, with a maximum of 25.0 µg/mL (Table 3). Over this concentration NR diffused in the Si-HPMC water phase and BPMGs formation was not possible anymore. This was ascribed to an increase of the microviscosity in the cellulosic hydrogel, due to the interactions with NR that disrupt the first layer of hydration (Katzhendler, *et al*., 2000). The size distribution of the oil droplets was also affected by the NR loading.

3.4. Mechanical properties of the FMGs and the BPMGs

The cross linking efficiency was evaluated by measuring the nanomechanical properties of the FMGs and the BPMGs by the means of atomic force microscopic nano indentation (Figure 5). In addition to the measurement of the hardness value, the depth-sensing indentation has been routinely used to extract the elastic properties of the specimen, with known indenter geometry and material properties. (Poon, *et al*., 2008) According to Sneddon's equation, the elastic modulus E (kPa) was calculated to give an indication of the hardness of the samples.

The elastic modulus of the FMGs was found to be 5.9 kPa which is two times higher than the value previously observed for cylindrical gels Si-HPMC-Si (∅ ≈ 2.4 cm) that was determined at 2.96 kPa by measuring their compressive modulus. (Rederstorff, *et al*., 2011) This confirmed the cross linking efficiency inside the microdroplets of the Si-HPMC W/O emulsion. The elastic modulus of the BPMGs was significantly increased up to 144 kPa due to the presence of the oily phase trapped inside the cross linked Si-HPMC hydrogel. There is a great increase in the elastic modulus which is an indication of its hardness. Sekine *et al.* reported that the hardness and stability of o/w/o multiple

340 emulsion was enhanced by increasing the weight ratio of the inner O/W emulsion. (Sekine, *et al.*,
341 2000)

342 These values match with elastic modulus of 2 to 204 kPa, that can be recorded on gelatin methacrylic
343 microgels ≤10 wt% with sizes in the same range (<5-150µm) and depending on the formulation
344 parameters. (Cha, *et al.*, 2014; Nguyen, *et al.*, 2015) As comparison, living cells exhibit elastic
345 modulus comprised in a range of 0.2 - 200 kPa that depends on the differentiation stage, growth,
346 adhesion. (Kuznetsova, *et al.*, 2007) Both the size and elastic modulus of the FMGs and the BPMGs
347 were comparable to those of eukaryotic living cells. This allows good expectations for their
348 coexistence in confined physiological environment, such as injectable or implantable scaffolds.

349 **3.5. Chemical and physical stability of FMGs and BPMGs**

350 Polysaccharide-based microgels with high water content, controllable particle size and high stability
351 have been widely studied as candidates for drug release and delivery. Different release mechanisms
352 of drugs could be observed from hydrogels. (Hamidi, *et al.*, 2008) The most common mechanism is
353 passive diffusion, meaning free diffusion into/out of the hydrogel network. It depends mainly on the molecular
354 size and the mesh size of the hydrogel network, and follows the Fick's first law of diffusion. Typical porosities
355 expressed in mesh size are reported for biomedical hydrogels in the range of 5 to 100 nm (in their swollen
356 state). After comparison, it could be related to the dimensions observed on the ladder size of the Si-HPMC
357 network (Figure 4D), which are much larger than most of small molecule drugs.

358 The release of the model drugs from BPMGs was evaluated in a phosphate buffer saline (PBS) at pH 7.4 and
359 37°C to mimic standard physiological conditions. After a period of 40 days, no diffusion of fluorescein was
360 observed indicating a stable linkage to the Si-HPMC (Figure 6). No diffusion in the external medium was
361 either observed for the Nile Red. The detection threshold was found to be in the range of 0.5 picoM both in
362 the PBS buffer and in DMSO. The intensities of fluorescence were in the same range from 1 µM and 25 µM
363 in both solvents. The maximum concentration of NR that could be released in the PBS was about 20 µM. So,
364 there was not a problem of detection of the NR in the aqueous medium. Moreover, some accumulation of NR
365 was observed in the Si-HPMC phase, as it can be seen in Figure 7 (B, D, F).

366 This was ascribed to a partition with the oil droplets, as described by Busatto *et al.* with progesterone
367 encapsulated in oil droplets trapped in microgels based on methacrylated hyaluronic acid. (Busatto, *et al*.,
368 2017) The NR behavior was hypothesized to adsorbed to the hydrophobic isopropyl and methyl parts of
369 HPMC. It is important to notice that this NR retention is not due to its poor water solubility but rather due to
370 the physical properties of the microgels. In fact, NR encapsulated in lipid nanoparticles (Delmas *et al*.,2012)
371 and either in nanoemulsions dispersed in chitosan hydrogel (Delmar *et al*., 2016) showed sustained but
372 complete releases.

373 After 17 days of incubation, however, microscopic observations exhibited a loss of the spherical structure and
374 a release of the oil droplets, accompanied by a loss of the mechanical properties, oil droplets were released
375 leaving empty skin structures of cross linked microgels (Figure 7C).

376 A full extraction with an organic solvent, DMSO, allowed the extraction of the fractions of fluorescein and
377 NR supposed to be adsorbed by weak interactions in the hydrogel. DMSO did not have hydrolytic action on
378 the Si-O-Si chemical bonds, but is able to solubilize all the components of the BPMGs namely sesame
379 oil, Nile Red, fluorescein and HPMC (Cao, *et al*., 2015). This resulted in the extraction of 85±7 wt.%
380 of the total initial amount of fluorescein. This means that about 15% of the fluorescein was still
381 linked to Si-HPMC matrix. About 70±7 wt.% of the initial amount of NR were also extracted (Figure
382 6).

383 Extreme values of pH (acidic pH 1.5 and alkaline pH 10.0) were applied to the BPMGs in order to evaluate
384 the chemical stability of the Si-O-Si bridges (Brinker, Scherer, 1990). The acidic conditions did not affect
385 the release. It was correlated to the strengthening of the mechanical properties of both BPMGs and
386 FMGs (Figure 7). This behavior could be related to self hardening process due to the condensation of
387 silanolates into siloxane bridges, which is promoted at low pH values (Bourges, *et al*., 2002b)
388 (Brinker & Scherer, 1990).

389 However, in alkaline conditions, 25±5 wt.% of the total amount of Si-Fluor and 15±3 wt.% of the
390 total amount of NR could be extracted. The release of these fractions was then subjected to the
391 degradation of the Si-O-Si bonds. A fraction of the Si-Fluor species were released by hydrolysis of

the Si-O-Si bond. The oil droplets trapping the NR could be released by the hydrolytic degradation of the Si-O-Si bonds involved in the Si-HPMC network. Actually, a good stability of the linkage of Si-Fluor to the Si-HPMC hydrogel was observed, which will be suitable for further biological functionalization of the FMGs and the BPMGs.

These results showed a strong retention of the model drugs, Si-Fluor and NR, in simulated physiological conditions. Therefore, the hydrophobic drug control release should be obtained under mechanical stimulation.

Conclusion

The preparation and the functionalization of microgels made of Si-HPMC were obtained by the unique condensation reaction of alkoxysilane functions in physiological conditions of temperature and pH. An emulsion templating process was applied using only the interfacial properties of HPMC without the use of any surfactant.

The size distributions of the microgels are relevant with injections in implant sites for intra-articular, sub-cutaneous.

The model function Si-Fluor was chemically linked with a good stability and in the range of amounts compatible with a further biological activity.

Biphasic microgels were obtained with a double emulsion process for the loading of a lipophilic model drug in oil droplets trapped in the hydrogel core. The oil droplets could be released after incubation in physiological conditions for 17 days. Mechanical stimulation will be needed to trigger further drug release.

Finally, it was shown that the alkoxysilane modified hydrogels represents a promising modular strategy that open a new way to design and to multi-functionalize drug delivery systems in limited preparation steps.

Authors contribution

M. Zayed, PhD fellowship, did the full preparation and characterizations of the materials. Prof. P. Weiss synthesized and provided the silylated HPMC. Prof. G. Subra and Prof. A. Mehdi synthesized and provided the silylated fluorescein. M. Ramonda performed the AFM measurements and Elastic modulus calculations. Prof. P. Legrand, Prof. J.-M. Devoisselle and Dr C. Tourne-Peteilh supervised the processing and characterizations of the elaboration of the microgels.

Acknowledgment: Misr University for Science and Technology (MUST), University of Egypt, for grant of Mr Mohamed Zayed PhD degree. LCSM observations were done on the Technology Facilities for Life Sciences, BioCampus, Montpellier, France.

Corresponding author : Dr C. Tourne-Peteilh, affiliated to University of Montpellier, Departement of Chemistry, ICGM, UMR 5253 CNRS-UM-ENSCM, Faculté de Pharmacie, 15 avenue Charles Flahault, Bât C, 3Et., 34093 Montpellier; *email :* corine.tourne-peteilh@enscm.fr; *tel :* +33 (0)4 11 75 94 52.

References

Ahmed, I. S., Hassan, M. A.-E., 2007. In vitro and in vivo evaluation of a fast-disintegrating lyophilized dry emulsion tablet containing griseofulvin. Eur. J. Pharm. Sci. 32, 58-68.

Bachman, H., Brown, A. C., Clarke, K. C., Dhada, K. S., Douglas, A., Hansen, C. E., *et al*., 2015. Ultrasoft, highly deformable microgels. Soft Matter. 11, 2018.

Bento da Silva, P., de Freitas, E. S., Bernegossi, J., Gonçalez, M. L., Sato, M. R., Leite, C. Q., *et al*, 2016. Nanotechnology-Based Drug Delivery Systems for Treatment of Tuberculosis—A Review. J. Biomed. Nanotechnol. 12, 241-260.

Borcoman, E., Le Tourneau, C., 2016. Antibody Drug Conjugates: The Future of Chemotherapy ? Curr. Opin. Oncol. 28, 429-436.

Bourges, X., Weiss, P., Coudreuse, A., Daculsi, G., Legeay, G., 2002. General Properties of Silated Hydroxyethylcellulose for Potential Biomedical Applications. Biopolymers. 63, 232-238.

Bourges, X., Weiss, P., Daculsi, G., & Legeay, G., 2002. Synthesis and general properties of silated-(hydroxypropyl)methyl cellulose in prospect of biomedical use. Adv. Colloid Interface Sci. 99, 215-228.

442 Bradshaw, C. S., & Sobel, J. D., 2016. Current Treatment of Bacterial Vaginosis - Limitations and Need for
443 Innovation. Proceedings of the 2015 NIH/NIAID Bacterial Vaginosis Expert Consultation. 214, S14-S20.
444 Brinker, J. C., & Scherer, G. W., 1990. Sol-Gel Science - The Physics and Chemistry of Sol-Gel Processing.
445 San Diego (USA), London (UK): Academic Press, Elsevier.
446 Buchtova, N., Rethore, G., Boyer, C., Guicheux, J., Rambaud, F., Valle, K., *et al*., 2013. Nanocomposite
447 hydrogels for cartilage tissue engineering: mesoporous silica nanofibers interlinked with siloxane derived
448 polysaccharide. J. Mater. Sci. Mater. Med. 24, 1875-1884.
449 Busatto, C., Labie, H., Lapeyre, V., Auzely-Velty, R., Perro, A., Casis, N., *et al*., 2017. Oil-in-microgel
450 strategy for enzymatic-triggered release of hydrophobic drugs. J. Colloid Interface Sci. 493, 356-364.
451 Cao, H., Song, J., Fang, X., 2015. Effect of dimethyl sulfoxide (DMSO) on cellulose solution with high
452 concentration. Adv. Mat. Res. 1095, 329-332.
453 Cha, C., Oh, J., Kim, K., Qiu, Y., Joh, M., Shin, S. R., *et al*., 2014. Microfluidics-Assisted Fabrication of
454 Gelatin-Silica Core−Shell Microgels for Injectable Tissue Constructs. Biomacromolecules. 15, 283−290.
455 Ciccione, J., Jia, T., Coll, J.-L., Parra, K., Amblard, M., Jebors, S., *et al*., 2016. Unambiguous and Controlled
456 One-Pot Synthesis of Multifunctional Silica Nanoparticles. Chem. Mater. 28, 885−889.
457 Colombo, M., Fiandra, L., Alessio, G., Mazzucchelli, S., Nebuloni, M., De Palma, C., *et al*., 2016. Tumour
458 homing and therapeutic effect of colloidal nanoparticles depend on the number of attached antibodies. Nat.
459 Commun. 7, 13818.
460 Dang, Q., Liu, C., Wang, Y., Yan, J., Wan, H., Fan, B., 2016. Characterization and biocompatibility of
461 injectable microspheres-loaded hydrogel for methotrexate delivery. Carbohydr. Polym. 136, 516–526.
462 Delmar, K., Bianco-Peleda, H., 2016, Composite chitosan hydrogels for extended release of hydrophobic
463 drugs, Carbohydrate Polymers, 136, 570-580.
464 Delmas, T., Fraichard, A., Bayle, P.-A., Texier, I. Bardet, M., Baudry, J. Bibette, J. and Couffin, A-C.,
465 2012, Encapsulation and Release Behavior from Lipid Nanoparticles: Model Study with Nile Red
466 Fluorophore, J. Colloid Sci. Biotechnol.1, 16-25
467 Echalier, C., Jebors, S., Laconde, G., Brunel, L., Verdie, P., Causse, L., *et al*., 2017. Sol–gel synthesis of
468 collagen-inspired peptide hydrogel. Mater. Today. 20, 59-66.

469 Echalier, C., Pinese, C., Garric, X., Van Den Berghe, H., Jumas Bilak, E., Martinez, J., *et al*., 2016. Easy
470 Synthesis of Tunable Hybrid Bioactive Hydrogels. Chem. Mater. 28, 1261-1265.
471 Fatimi, A., & Tassin, J.-F., 2009. Gelation studies of a cellulose-based biohydrogel: Influence of pH,
472 temperature and sterilisation. Acta Biomater. 5, 3423-3432.
473 Fatimi, A., Tassin, J.-F., Quillard, S., Axelos, M. A., Weiss, P., 2008. The rheological properties of silated
474 (hydroxypropyl)methyl cellulose tissue engineering matrices. Biomaterials. 29, 533-543.
475 Glaubitz, M., Medvedev, N., Pussak, D., Hartmann, L., Schmidt, S., Helm, C. A., *et al*., 2014. A novel contact
476 model for AFM indentation experiments on soft spherical cell-like particles. Soft Matter. 10, 6732.
477 Hamidi, M., Azadi, A., Rafiei, P., 2008. Hydrogel nanoparticles in drug delivery. Adv. Drug Deliv. Rev. 60,
478 1638–1649.
479 Jagadeesan, D., Nasimova, I., Gourevich, I., Starodubtsev, S., Kumacheva, E., 2011. Microgels for the
480 Encapsulation and Stimulus-Responsive Release of Molecules with Distinct Polarities. Macromol. Biosci. 11,
481 889-896.
482 Katzhendler, I., Mader, K., Friedman, M., 2000. Structure and hydration properties of (hydroxypropyl)methyl
483 cellulose matrices containing naproxen and naproxen sodium. Int. J. Pharm, 200, 161-179.
484 Kelkar, S. S., Reineke, T. M., 2011. Theranostics: Combining Imaging and Therapy. Bioconjugate Chem. 22,
485 1879-2198.
486 Küchler, S., Abdel-Mottaleb, M., Lamprecht, A., Radowskic, M. R., 2009. Influence of nanocarrier type and
487 size on skin delivery of hydrophilic agents. Int. J. Pharm. 377, 169-172.
488 Kuznetsova, T. G., Starodubtseva, M. N., Yegorenkov, N. I., Chizhik, S. A., Zhdanov, R. I., 2007. Atomic
489 force microscopy probing of cell elasticity. Micron. 38, 824-833.
490 Le Douce, V., Ait-Amar, A., Forouzan far, F., Fahmi, F., Quiel, J., El Mekdad, H., *et al*., 2016. Improving
491 combination antiretroviral therapy by targeting HIV-1 gene transcription. Expert Opin. Ther. Targets. 20,
492 1311-1324.
493 Liu, W., Zhang, J., Rethore, G., Khairoun, K., Pilet, P., Tancret, F., 2014. A novel injectable, cohesive and
494 toughened Si-HPMC (silanized-(hydroxypropyl)methyl cellulose) composite calcium phosphate cement for
495 bone substitution. Acta Biomater. 10, 3335-3345.

496 Marquis, M., Alix, V., Capron, I., Cuenot, S., Zykwinska, A., 2016. Microfluidic Encapsulation of Pickering
497 Oil Microdroplets into Alginate Microgels for Lipophilic Compound Delivery. ACS Biomater. Sci. Eng. 2,
498 535-543.
499 Marquis, M., Davy, J., Fang, A., Renard, D., 2014. Microfluidics-Assisted Diffusion Self-Assembly: Toward
500 the Control of the Shape and Size of Pectin Hydrogel Microparticles. Biomacromolecules. 15, 1568-1578.
501 Matalanis, A., McClements, D. J., 2013. Hydrogel microspheres for encapsulation of lipophilic components:
502 Optimization of fabrication & performance. Food Hydrocoll. 31, 15-25.
503 Matalanis, A., Griffith Jones, O., McClements, D. J., 2011. Structured biopolymer -based delivery systems for
504 encapsulation, protection, and release of lipophilic compounds. Food Hydrocoll. 25, 1865-1880.
505 Merian, J., Gravier, J., Navarro, F., Texier, I., 2012. Fluorescent Nanoprobes Dedicated to in Vivo Imaging:
506 From Preclinical Validations to Clinical Translation. Molecules. 17, 5564-5591.
507 Morgan, C. E., Wasserman, M. A., Kibbe, M. R., 2016. Targeted Nanotherapies for the Treatment of Surgical
508 Diseases. Ann. Surg. 263, 900-907.
509 Moussa, L., Pattappa, G., Doix, B., Benselama, S.-L., Demarquay, C., Benderitter, M., *et al*., 2017. A
510 biomaterial-assisted mesenchymal stromal cell therapy alleviates colonic radiation-induced damage.
511 Biomaterials. 115, 40-52.
512 Nguyen, A. H., McKinney, J., Miller, T., Bongiorno, T., McDevitt, T. C., 2015. Gelatin methacrylate
513 microspheres for controlled growth factor release. Acta Biomater. 13, 101-110.
514 Pagels, R. F., & Prud'homme, R. K., 2015. Polymeric nanoparticles and microparticles for the delivery of
515 peptides, biologics, and soluble therapeutics. J. Control. Release. 219, 519-535.
516 Pallicer, J. M., Roses, M., Rafols, C., Bosch, E., Pascual, R., Port, A., 2014. Evaluation of log Po/w values of
517 drugs from some molecular structure calculation software. ADMET & DMPK. 2, 107-114.
518 Poon, B., Rittel, D., Ravichandran, G., 2008. An analysis of nano indentation in linearly elastic solids. Int. J.
519 Solids Struct., 6018-6033.
520 Popp, I., Del Pozzo, L., Waser, B., Reubi, J. C., Meyer, P. T., 2017. Approaches to improve metabolic
521 stability of a statine-based GRP receptor antagonist. Nucl. Med. Biol. 45, 22-29.
522 Pyka, A., Babuska, M., & and Zachariasz, M., 2006. A comparison of theoretical methods of calculation of
523 partition coefficients for selected drugs. Acta Pol. Pharm. 63, 159-167.

524 Rederstorff, E., Weiss, P., Sourice, S., Pilet, P., Xie, F., Sinquin, C., *et al*., 2011. An in vitro study of two
525 GAG-like marine polysaccharides incorporated into injectable hydrogels for bone and cartilage tissue
526 engineering. Acta Biomater. 7, 2119-2130.
527 Rowe, R. C., Sheskey, P. J., & Quinn, M. E., 2009. Handbook of Pharmaceutical Excipients Sixth edition.
528 UK, USA: Pharmaceutical Press and the American Pharmacists Association.
529 Rui, M., Qu, Y., Gao, T., Ge, Y., Feng, C., Xu, X., 2017. Simultaneous delivery of anti-miR21 with
530 doxorubicin prodrug by mimetic lipoprotein nanoparticles for synergistic effect against drug resistance in
531 cancer cells. Int. J. Nanomedicine. 12, 217-237.
532 Sekine, T., Yoshida, K., Matsuzaki, F., Yanaki, T., Yamaguchi, M., 2000. A Novel Method for Preparing Oil-
533 in-Water-in-Oil Type Multiple Emulsions Using Organophilic Montmorillonite Clay Mineral. J. Surfactants
534 Deterg. 2, 309-315.
535 Struillou, X., Rakic, M., Badran, Z., Macquigneau, L., Colombeix, C., Pilet, P., *et al*., 2013. The association
536 of hydrogel and biphasic calcium phosphate in the treatment of dehiscence-type peri-implant defects: an
537 experimental study in dogs. J. Mater. Sci. Mater. Med. 24, 2749-2760.
538 Subbiah, R., Hwang, M. P., Van, S. Y., Do, S. H., Park, H., 2015. Osteogenic/Angiogenic Dual Growth Factor
539 Delivery Microcapsules for Regeneration of Vascularized Bone Tissue. Adv. Healthc. Mater. 4, 1982-92.
540 Teo, P. Y., Cheng, W., Hedrick, J. L., Yan, Y., 2016. Co-delivery of Drugs and Plasmid DNA for Cancer
541 Therapy. Adv. Drug Deliv. Rev. 98, 41-63.
542 Ulbrich, K., Hola, K., Subr, V., Bakandritsos, A., Tucek, J., Zboril, R., 2016. Targeted Drug Delivery with
543 Polymers and Magnetic Nanoparticles: Covalent and Noncovalent Approaches, Release Control, and Clinical
544 Studies. Chem. Rev. 116, 5338-5431.
545 Vinatier, C., Gauthier, O., Fatimi, A., Merceron, C., Masson, M., Moreau, A., et al. (2009). An Injectable
546 Cellulose-Based Hydrogel for the Transfer of Autologous Nasal Chondrocytes in Articular Cartilage Defects.
547 Biotechnology and Bioengineering , 102 (4), 1259-1267.
548 Vinatier, C., Magne, D., Moreau, A., Gauthier, O., Malard, O., Vignes-Colombeix, C., *et al*., 2007.
549 Engineering cartilage with human nasal chondrocytes and a silanized (hydroxypropyl)methyl cellulose
550 hydrogel. J. Biomed. Mater. Res. A, 80A, 66-74.

551 Vinatier, C., Mrugala, D., Jorgensen, C., Guicheux, J., & Noël, D. (2009). Cartilage engineering: a crucial
552 combination of cells, biomaterials and biofactors. Trends in Biotechnology , 27 (5), 307-314.
553 Weber, M., Zoschke, C., Sedighi, A., Fleige, E., Haag, R., Schäfer-Korting, M., 2014. Free Energy
554 Simulations of Cargo-Carrier Interactions for Core-Multishell Nanotransporters. J. Nanomed. Nanotechnol., 5,
555 1000234.
556 Wollenweber, C., Makievski, A., Miller, R., Daniels, R., 2000. Adsorption of (hydroxypropyl)methyl
557 cellulose at the iquid/liquid interface and the effect on emulsion stability. Colloids Surf. A Physicochem. Eng.
558 Asp. 172, 91-101.
559 Wu, S., Yang, X., Li, W., Du, L., Zeng, R., Tu, M., 2017. Enhancing osteogenic differentiation of MC3T3-E1
560 cells by immobilizing RGD onto liquid crystal substrate. Mater. Sci. Eng. C Mater. Biol. Appl. 71, 973-981.
561 Zhang, J., Liu, W., Gauthier, O., Sourice, S., Pilet, P., Rethore, G., *et al*., 2016. A simple and effective
562 approach to prepare injectable macroporous calcium phosphate cement for bone repair: Syringe-foaming using
563 a viscous hydrophilic polymeric solution. Acta Biomate. 31, 326-338.
564 Zhao, C.-X. (2013). Multiphaseflow microfluidics for the production of single or multiple emulsions for drug
565 delivery. Adv. Drug Deliv. Rev. 65, 1420-1446.

*Graphical Abstract (for review)

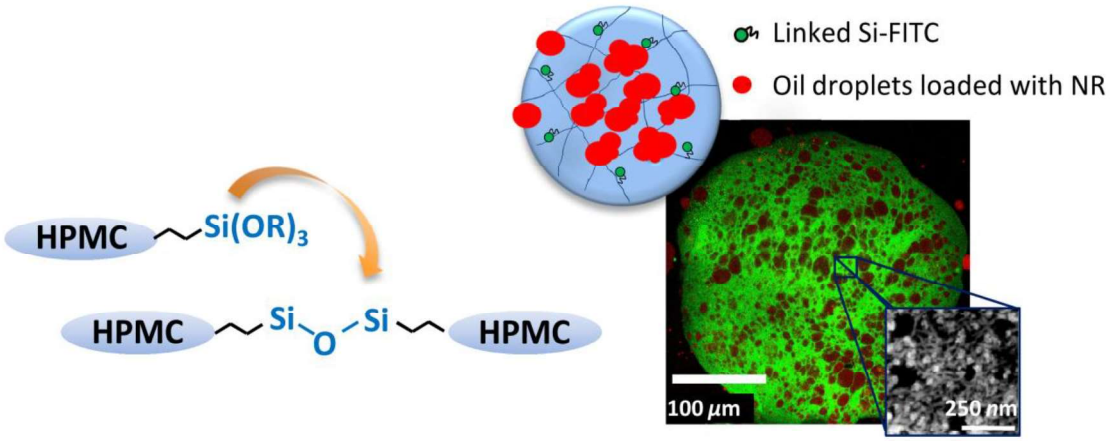

List of table and figure caption
Click here to view linked References

Scheme 1: This scheme represents the protocol of preparation of FMGs and BPMGs based on the sol-gel reaction and a templating emulsification process. The pH and the temperature are the main parameters that control the chemical cross-linking reaction, leading to formation of Si-O-Si bonds. The Si-HPMC network could be functionalized with a model molecule, such as Si-FITC in FMGs. Oil compartments for lipophilic molecules encapsulation, were trapped in the BPMGs.

Table 1: Interfacial behavior of Si-HPMC versus HPMC.

Figure 1: Emulsions W/O of Si-HPMC (A) leads to the formation of the microgels only after neutralization and increasing the temperature to 45°C (B), while no spherical morphologies were obtained at pH 12 and room temperature (C). HPMC W/O emulsion (D) did not give any structures after pH and temperature treatment (pH neutralization, T°C = 45°C) (E). (bar = 400 µm)

Figure 2: Optimization of the size distribution of the microgels by adjusting the water phase in oil feeding rate, for the microgels W/O (A) and BPMGs O/W/O (B, C, D). The red curve is the Log Normal fit. (bar = 400 µm)

Table 2: Loading efficiency of Si-Fluor determined in bulk hydrogel (C_I = initial weight concentration; C_L = linked weight concentration).

Figure 3: (A) Optical microscopy of the first dispersion O/W (O = sesame oil; W = Si-HPMC 3wt%, (B) Size distribution of the oil droplets (log normal fitting curve), (C) Phase separation between the oil droplets phase (Nile Red labeling) dispersed in Si-HPMC 3 wt% sol labeled with Si-Fluor by LCSM, (D) SEM of the freeze-dryed O/W emulsion.

Table 3: Loading efficiency of Nile red in the oily phase, effect on the size distribution of the oil droplets and of the BPMGs

Figure 4: SEM observations of (A) hydrated and (B) freeze-dried BPMGs, their internal phase separation (C) between the hydrophilic and the lipophilic phases by LSCM, and the topography (D) of the Si-HPMC network of dried BPMGs determined by AFM.

Figure 5: AFM nanoindentation on FMGs (black) and BPMGs (red) reporting the Force (N) to indentation distance fitted by the Sneddon model.

Figure 6: Effect of physiological and extreme pH on the extraction and release evaluation of the model drugs from the BPMGs.

Figure 7: Mechanical properties evolution of BPMGs with their optical microscopy (A, C, E) and epifluorescence (B, D, F) observations at different times of incubation : (A, B) BPMGs at D_0, (C, D) after 17 days in PBS 60 mM pH 7.4, (E, F) after 17 days in HCl pH 1.5. bar = 200 µm

Scheme 1

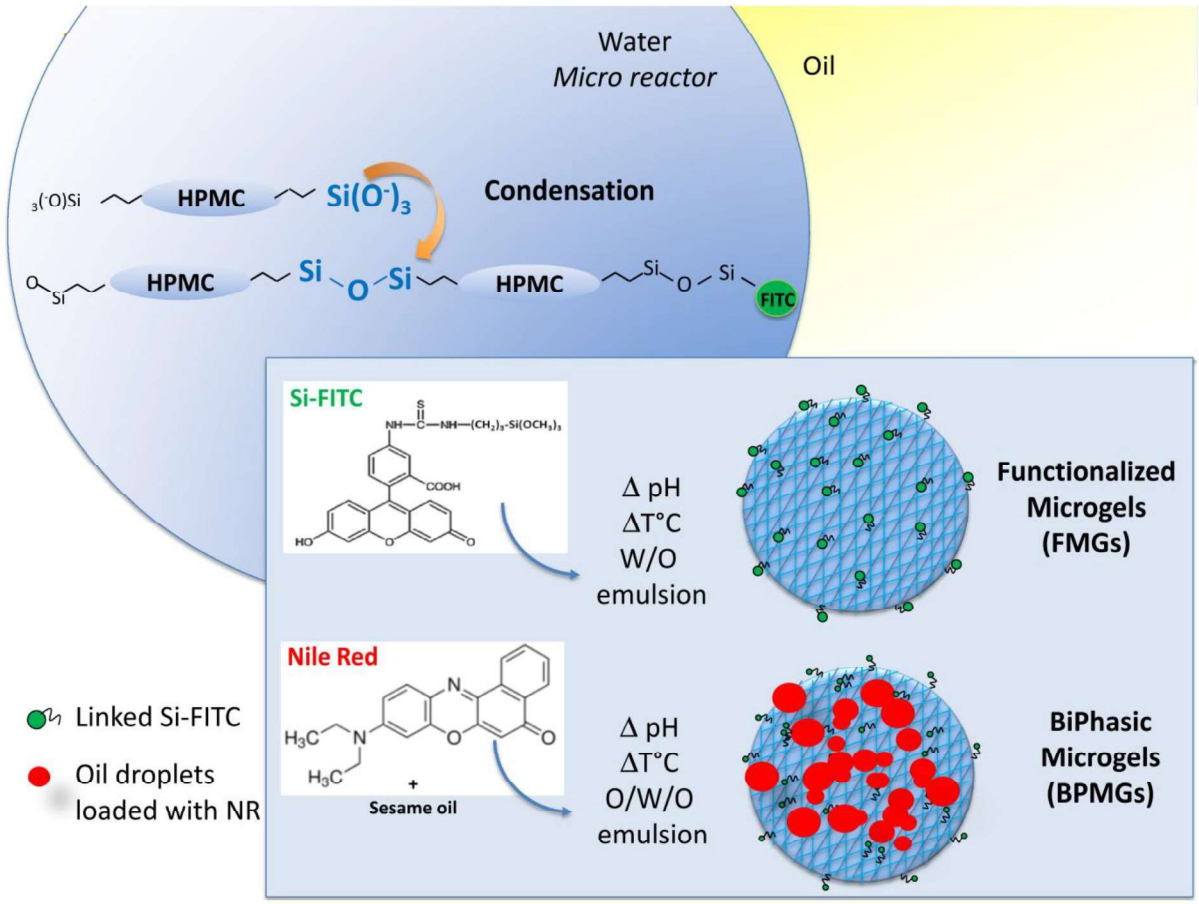
Water
Micro reactor
Oil
HPMC
Si(O-)3
Condensation
HPMC
Si
O
Si
HPMC
Si
O
Si
FITC
Si-FITC
Δ pH
ΔT°C
W/O
emulsion
Functionalized
Microgels
(FMGs)
Nile Red
Sesame oil
Δ pH
ΔT°C
O/W/O
emulsion
BiPhasic
Microgels
(BPMGs)
Linked Si-FITC
Oil droplets
loaded with NR

Table 1

	Γ (mol/m²)	CAC (M)	A_{Gibbs} (nm²)
HPMC 2910 [38]	$6.9\ 10^{-6}$	$1.82\ 10^{-7}$	0.24
Si-HPMC	$5.4\ 10^{-6}$	$5.40\ 10^{-8}$	0.31

Figure 1

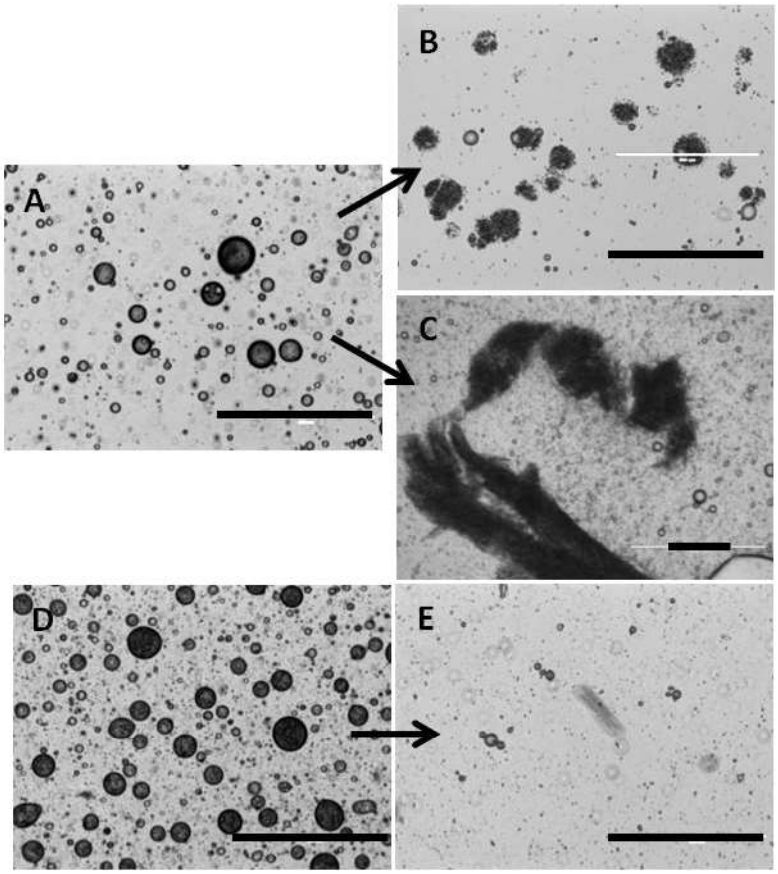

Figure 2

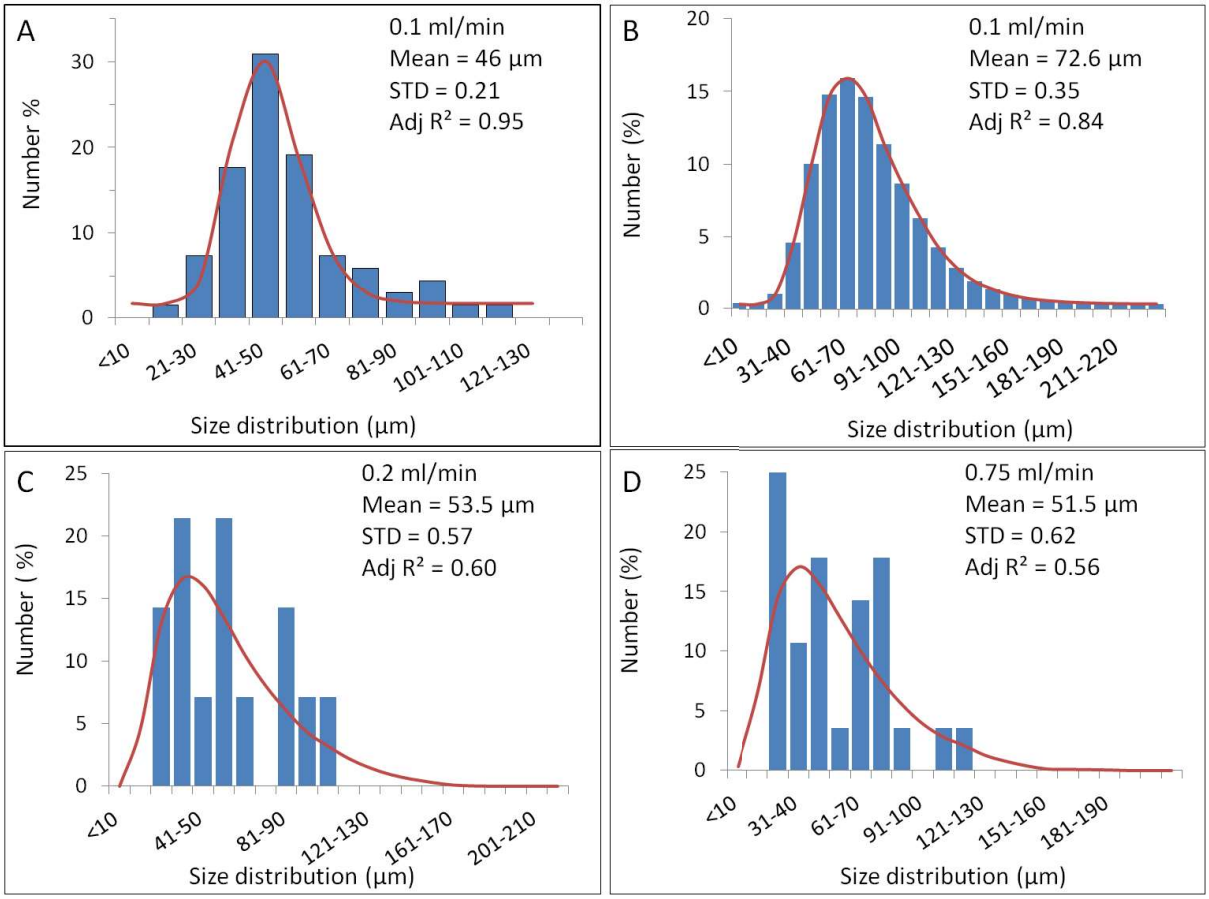
A
0.1 ml/min
Mean = 46 µm
STD = 0.21
Adj R² = 0.95
Number %
<10
21-30
41-50
61-70
81-90
101-110
121-130
Size distribution (µm)
B
0.1 ml/min
Mean = 72.6 µm
STD = 0.35
Adj R² = 0.84
Number (%)
<10
31-40
61-70
91-100
121-130
151-160
181-190
211-220
Size distribution (µm)
C
0.2 ml/min
Mean = 53.5 µm
STD = 0.57
Adj R² = 0.60
Number (%)
<10
41-50
81-90
121-130
161-170
201-210
Size distribution (µm)
D
0.75 ml/min
Mean = 51.5 µm
STD = 0.62
Adj R² = 0.56
Number (%)
<10
31-40
61-70
91-100
121-130
151-160
181-190
Size distribution (µm)

Table 2

C_i (µg /g HPMC-Si)	C_L (µg/g HPMC-Si)
0.09	0.09
0.45	0.44
1.12	1.12
2.23	0.73
11.12	0.80

Figure 3

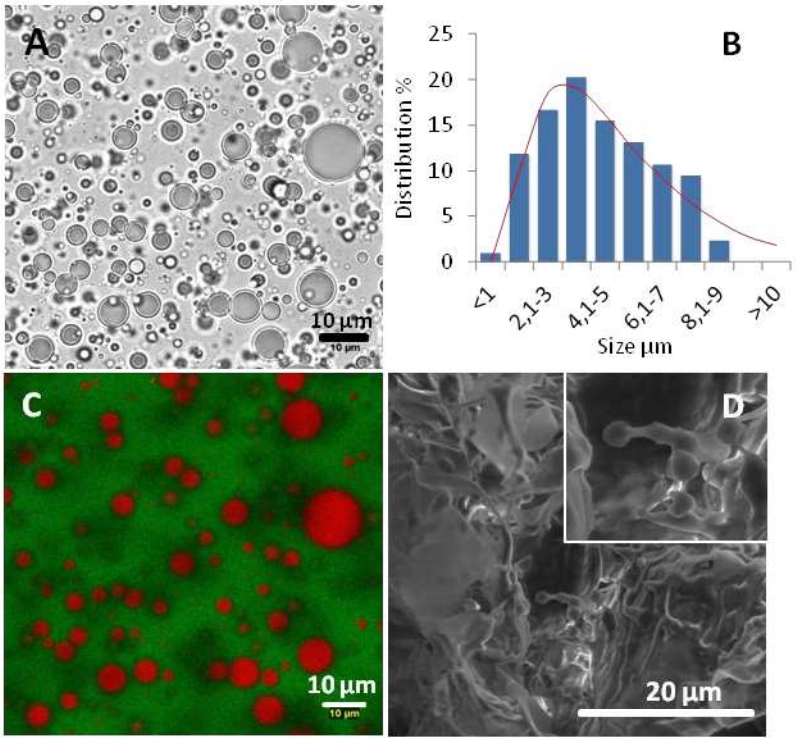
A
10 µm
B
Distribution %
25
20
15
10
5
0
<1
2,1-3
4,1-5
6,1-7
8,1-9
>10
Size µm
C
10 µm
D
20 µm

Table 3

Concentration in the oil phase (µg/ml)	O/W oil droplets		BPMGs	
	Size (µm)	STD (%)	Size (µm)	STD (%)
7.0	9.4	0.40	84.2	25
25.0	4.1	0.15	81.1	24
62.0	7.3	0.20	127.7	35
≥ 124.0	5.7	0.10	No BPMGs	No BPMGs

Figure 4

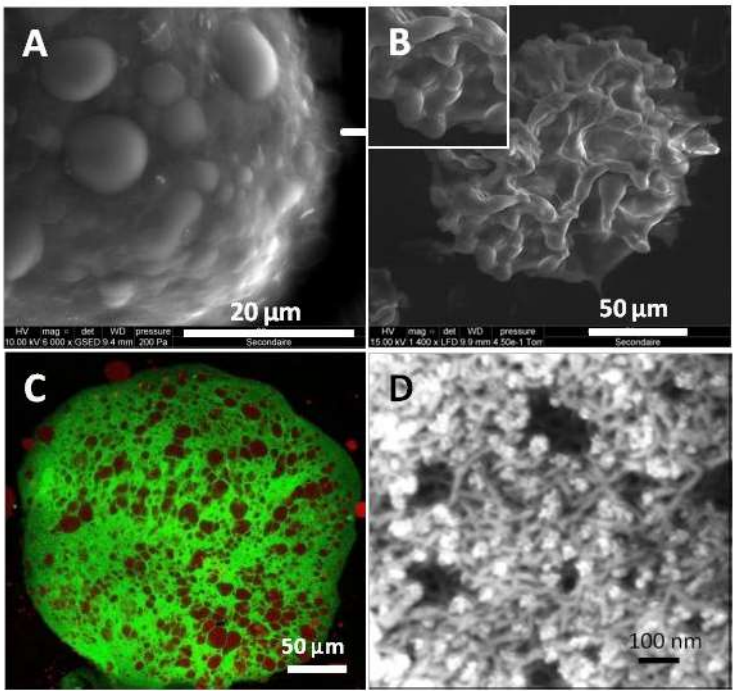

Figure 5

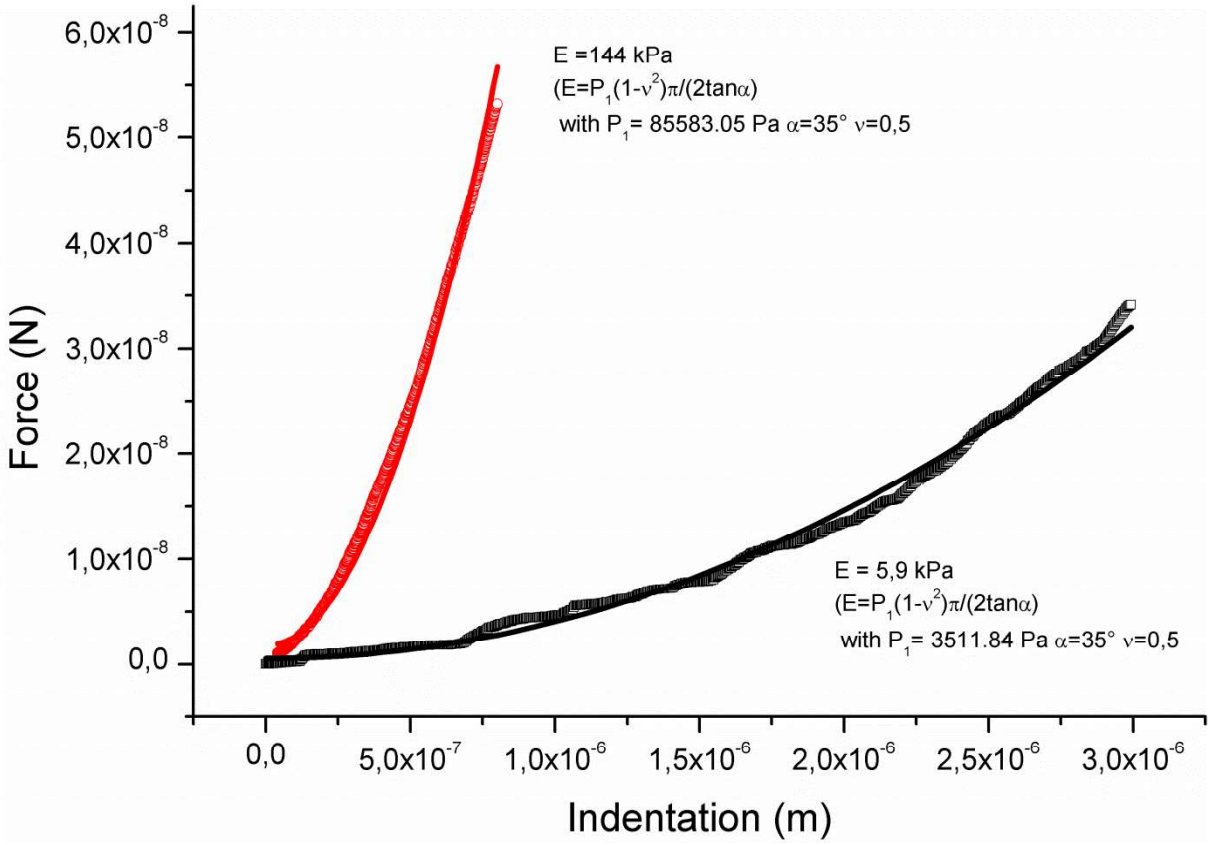
E =144 kPa
(E=P1(1-ν2)π/(2tanα)
with P1= 85583.05 Pa α=35° ν=0,5
E = 5,9 kPa
(E=P1(1-ν2)π/(2tanα)
with P1= 3511.84 Pa α=35° ν=0,5
Force (N)
6,0x10-8
5,0x10-8
4,0x10-8
3,0x10-8
2,0x10-8
1,0x10-8
0,0
0,0
5,0x10-7
1,0x10-6
1,5x10-6
2,0x10-6
2,5x10-6
3,0x10-6
Indentation (m)

Figure 6

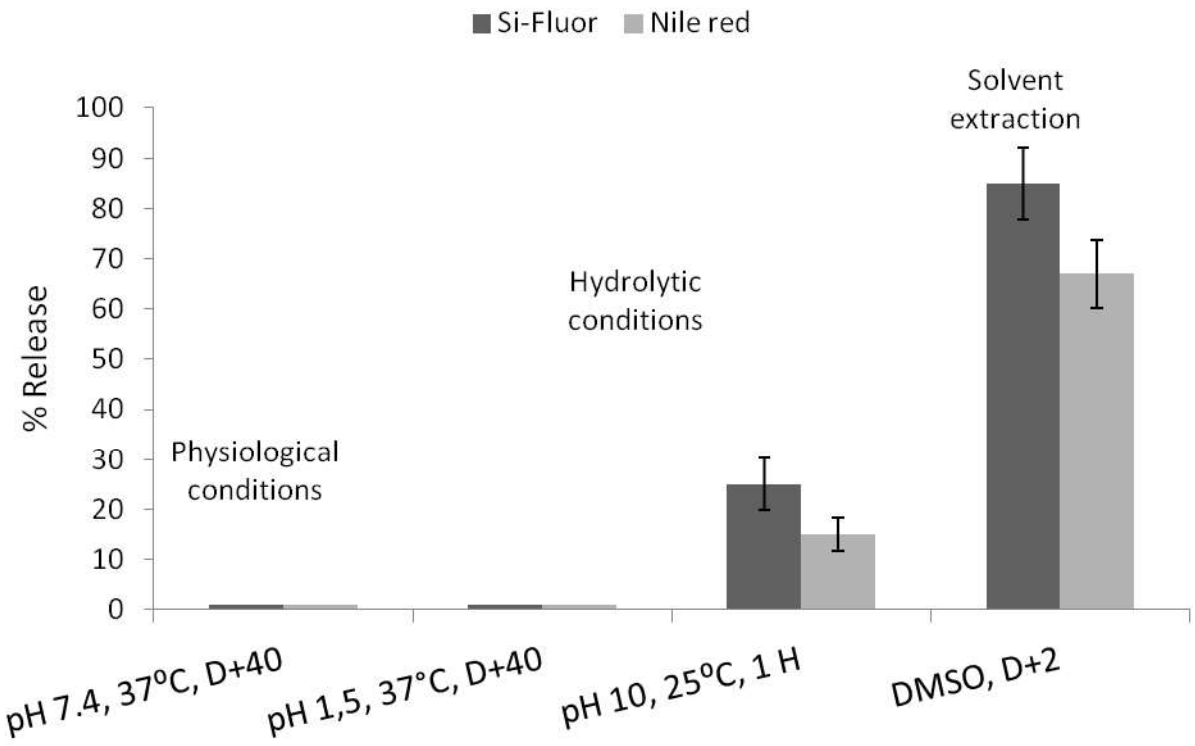
Si-Fluor
Nile red
% Release
100
90
80
70
60
50
40
30
20
10
0
Physiological conditions
Hydrolytic conditions
Solvent extraction
pH 7.4, 37°C, D+40
pH 1,5, 37°C, D+40
pH 10, 25°C, 1 H
DMSO, D+2

Figure 7

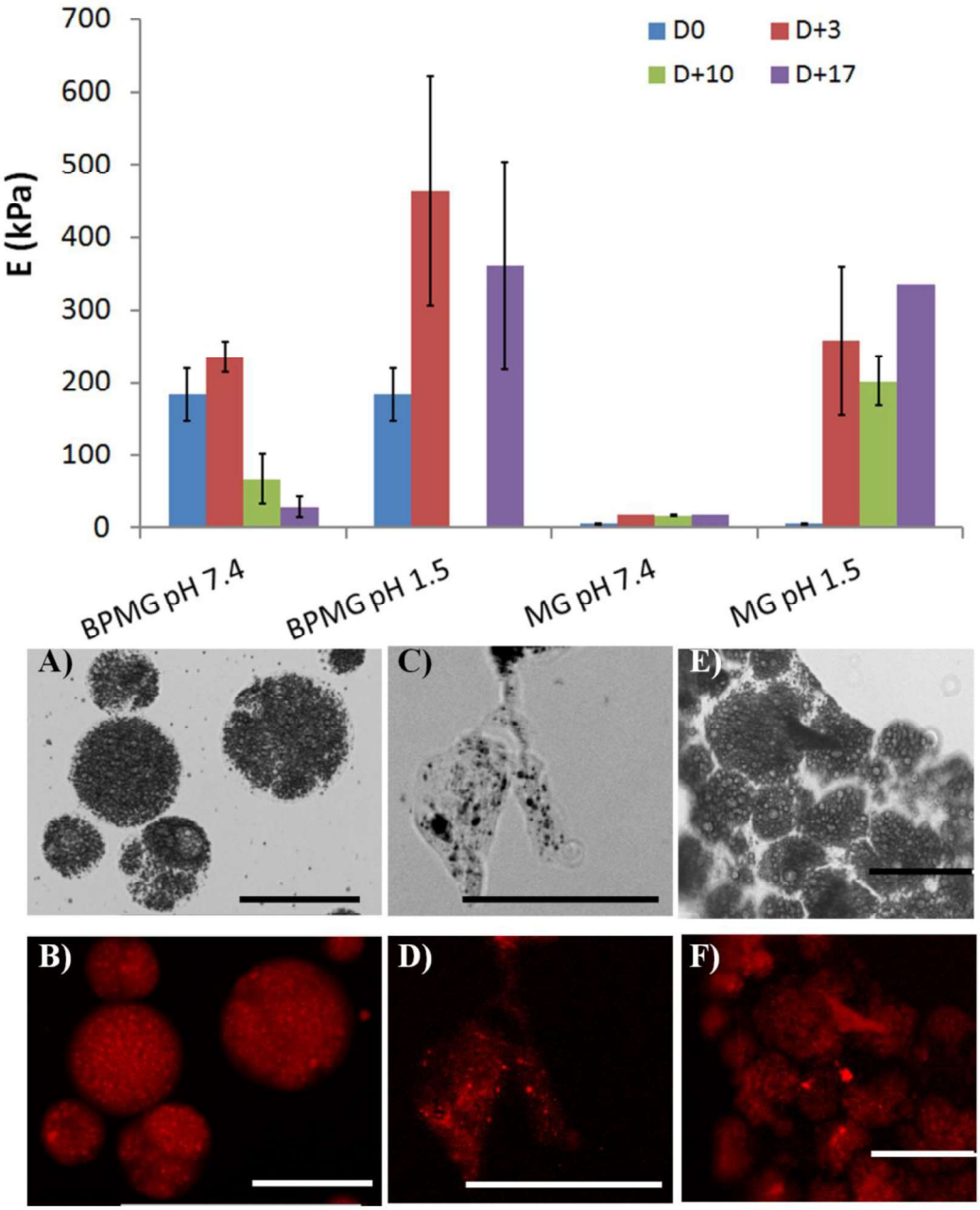
700
600
500
400
300
200
100
0
E (kPa)
D0
D+3
D+10
D+17
BPMG pH 7.4
BPMG pH 1.5
MG pH 7.4
MG pH 1.5
A)
C)
E)
B)
D)
F)